

The observed structures in the meteoroid stream of Perseids in the range of photographic meteors

Z. Kaňuchová, J. Svoreň and L. Neslušan

*Astronomical Institute of the Slovak Academy of Sciences
059 60 Tatranská Lomnica, The Slovak Republic*

Received: March 29, 2005; Accepted: July 27, 2005

Abstract. The activity of the Perseid stream in the range of photographic meteors is reviewed. An attention is paid to the activity of the stream close to the parent-comet return in 1991 to 1994, characteristics of the so-called *new maximum* and two different dust components – blanket in the present node of the comet and a ribbon-like structure, named as Nodal Blanket (Jenniskens et al., 1998) and Perseid Filament (Lindblad and Porubčan, 1994), respectively.

A fine structure of the Perseid stream and its filaments is studied using the method of indices - the procedure based only on mathematical statistics. In the study the new completed 2003 version of the IAU Meteor Data Center catalogue of precise photographic orbits (Lindblad et al., 2005) is employed. 560 (64%) of 875 Perseids taken into account were sorted out to 17 filaments found. The selected filaments are not distributed in the space accidentally, but they form higher structures consisting of 1 individual filament, 3 branches of the stream containing 9 filaments together and a central part of the stream. In the central part of Perseids, 3 branches and 1 individual filament were identified. The structures are divided into a cloud of 315 dispersed orbits.

Positions of 17 filaments are compared with strong mean-motion resonances with Jupiter and Saturn. The existence of gaps in the distribution of the semi-major axes of the Perseids is confirmed using the considerably more numerous material.

Key words: Perseids – structure of the meteoroid stream – photographic meteor orbits

1. Introduction

1.1. Definition of lengthwise and crosswise structures

The activity of the stream and its variation is a consequence of at least two factors, which blend each other. The first one is a varying spatial density of particles along the trajectory of the stream, it means the existence of the clusters of particles in the orbit, which give rise to shorter or longer-lived outbursts of meteors – lengthwise structures. The second one is a varying spatial density of

particles in the direction perpendicular to the motion vector, which is almost time independent. It is caused by an existence of fine crosswise patterns in the filamentary structure.

It is evident that these two forms of structures are merely two individual evolutionary stages transforming gradually the first into the second, under common conditions. A cloud of particles, observed as an increase of their spatial density at the beginning, can be formed as a consequence of higher activity at the perihelion (mostly) or, also, in another point of the cometary orbit, e.g. from a secondary source (as it was detected by Porubčan et al. (1992) during the outburst of Lyrids in 1982). Regardless of the place of origin, the particles disperse along the orbit of the comet in a short time and form a new or replenish some existing filament. A longer-period conservation of the lengthwise structure could occur, if the resonances with giant planets preserve the natural evolution of the stream (Williams, 1997; Jenniskens et al., 1998).

1.2. Reason for using photographic database

The changing activity of Perseids has been observed in all mass intervals, which pertain to individual observation methods (radar, visual and photographic). There were made many studies of an activity profile – for example Brown and Rendtel (1996) visually; Šimek (1987) by radar and so on.

However, if we want to define a source of this varying activity, i.e. to reveal the structure of the stream before its encounter with the Earth, we need to define atmospheric and subsequently heliocentric meteoroid orbits. The visual observations are hardly suitable for this purpose (because of a low precision of derived parameters). Radar orbits can be used assuming that the greater inaccuracy of individual orbits is compensated by their statistically sufficient amount. Hence we use the photographic orbits from IAU Meteor Data Center (MDC) database. In spite the fact that the photographic orbits used to be determined with the best accuracy, the differences between individual observing stations and programmes may be significant.

The Perseids have a high proportion of bright trailed meteors, making this stream very suitable for a study by photographic techniques (Evans, 1990). Also, the fact that the Perseids are preferred by observers (due to the summer season), causes that the stream is the most abundant one in the database.

1.3. Connection of the stream structures with a distribution of initial meteoroids velocities

Harris et al. (1995) noted that including both pre- and post-perihelion ejection is tantamount to assuming that the mass loss from the comet, and thus its heliocentric magnitude variation, is symmetrical with respect to the perihelion. This assumption is reasonable as Green (1993) found no obvious asymmetry on either side of perihelion in the visual light curve of comet 109P/Swift-Tuttle,

indicating that the comet may indeed outgas in a symmetric fashion with respect to the perihelion passage.

Wu and Williams (1995) demonstrated, by using the distribution of orbital energy as a vector in Markov process, that all memory of the initial distribution has been lost after a sufficiently long time, so that a very long-term evolution is governed by the effect of gravitational perturbation and radiation pressure. They also found that a trend is to move the distribution towards smaller values of the semi major axis. This is hardly surprising since there is an energy dissipation in the system through the inclusion of the Poynting-Robertson drag. A second effect giving rise to the same apparent trend is the loss of meteoroids on orbits of a large semi-major axis to hyperbolic orbits. This means that long-term structures might not be affected by initial conditions (particles' velocity distribution) to a large extent.

2. Lengthwise structures

2.1. Character of activity of the stream

The Perseid meteor shower is amongst the strongest and best known meteor showers currently visible from the Earth. The prolific activity of the shower coupled with its occurrence during summer in the northern hemisphere has made it among the best watched of astronomical events. The shower is recurring each year. The display lasts approximately one month, roughly from the half of July till the second decade of August. The definite intervals differ slightly according to various authors. Let us present some examples. On the basis of the visual observations held at the Skalnaté Pleso Observatory during 1944–1953 it has been found that the stream is active from July 20th to August 21st (Zvolánková, 1984). Wright and Whipple (1953) determined the interval of 28 days, July 28th–August 24th. According to Lindblad (1987) and Cook (1973), the activity period spans from July 25th to August 23rd and July 23rd–August 22nd, respectively. According to Svoreň et al. (1997), Perseids can be observed from July 12th to as late as September 9th.

2.1.1. The pre-perihelion period

The Perseids used to be a regular periodic shower, showing one maximum near August 12th with *Zenith Hour Rate* slightly varying between about 50 and 80 meteors (Hughes, 1990; Jenniskens, 1994). The typical profile of activity is shown in Fig. 1, which illustrates the results of analysis of visual observations during the years from 1953 to 1981 (Lindblad, 1986).

A couple of more outstanding exceptions have been recorded in the past (see reference in Kronk, 1988 or Hasegawa, 1993). Figure 2 shows the observations of the visual maximum of *Zenith Hour Rate* for the years from 1960 to 1962 and from 1975 to 1991 (Olson, 1992). According to Jenniskens (1994), careful

considering instrumental effects and statistical errors tend to find that *the peak annual rate* varies by only 20% or so, with no significant changes over a smooth and featureless activity profile. The remarkable 1991 maximum occurs at the beginning of the maxima sequence which was observed in the period around the last return of the parent comet.

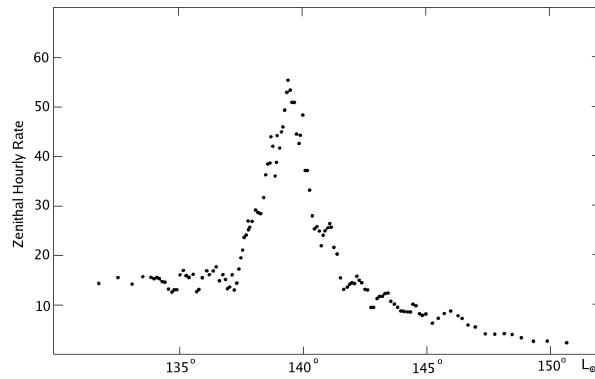


Figure 1. Perseid zenithal hourly rate versus solar longitude – sliding mean of 5 data points (Lindblad, 1986).

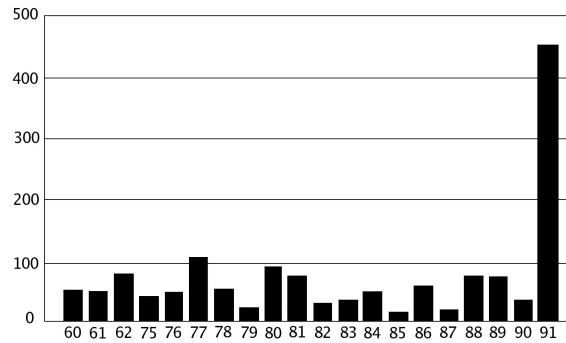


Figure 2. The maximum zenithal hour rate observed each year plotted as a function of the year for the periods from 1960 to 1962 and 1975 to 1991 (Olson, 1992). Notice the enhanced activity in 1991.

2.1.2. Activity of the stream close to the parent-comet return

Unusual activity of the Perseid shower has been confirmed for the years around the return of the comet to perihelion, which happened in December 1992. Roggemans' (1989) detection of a brief increase of rate during the 1988 display has often been credited as the first sign of this unusual activity, but this result has remained in doubt (Jenniskens et al., 1998).

Each year, the location and activity of the peak varied (Jenniskens et al., 1998). Before the perihelion passage, the time of maximum shifted towards the comet node at $\lambda_{\odot} = 139,445^{\circ}$ (Yau et al., 1994), as reported by Brown and Rendtel (1996). After the perihelion passage, the position of maximum shifted back to the asymptotic value obtained from photographically observed Perseids tens of years prior to perihelion (Lindblad and Porubčan, 1994).

The Perseid outbursts in 1991–1994 are referred to by Jenniskens (1995) as *near-comet outburst*. These outbursts are associated with the return of the comet to perihelion, meaning that they only occur when the comet itself returns to perihelion. The most remarkable feature of near-comet-type outbursts is the concentration of dust near the comet position. The Perseid activity in the referred period is considered as unusual not only because of a high value of the maximum hourly rate, but also due its appearance about 6 hours before the traditional maximum as well. So, the activity profile has considerably changed.

The old and new maxima were characterised by a very similar activity in the years 1988 and 1989. The new maximum was detected at $\lambda_{\odot} = 139.78^{\circ}$, about 6 hours before the traditional peak, which took place at $\lambda_{\odot} = 140.08^{\circ}$ (Roggemans, 1989; Koschack and Roggemans, 1991; Brown and Rendtel, 1996). The activity took only an hour.

There is a problem to establish the exact year of "breakpoint" in the activity because of data processing and their analysis. The information loss and resulting discrepancies can be a consequence of smoothing out the data by using a sliding mean or a too wide interval in the solar longitude as well. The importance of solar longitude interval width (as time variable) for the final activity profile demonstrates Lindblad's and Porubčan's (1994) study of 605 photographic Perseids. The study shows that the derived activity profile of the stream strongly depends on the resolution in the solar longitude used by the investigator. If the activity profile is investigated at a high resolution in the solar longitude, two distinct Perseid maxima appear, one at solar longitude 138.97° and the other at 139.61° (see Fig. 3). A more detailed investigation shows that the Perseid maximum has gradually changed with time, being located at approximately 139.5° – 139.6° in the period 1940–1969 and at 138.9° – 139.0° in the period 1970–1989.

Concerning the activity, the new maximum was comparable to the old one till 1991 (Jenniskens et al., 1998). In this year, the situation changed and the ZHR of the new maximum became more than 2.5 times higher than the ZHR of the traditional one.

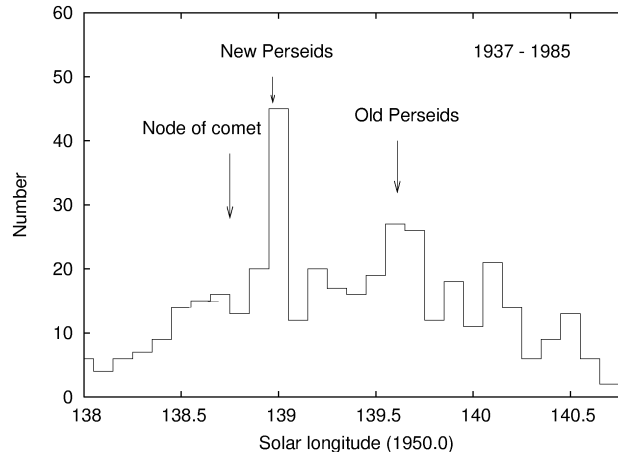


Figure 3. The number of photographic Perseids 1937–1985 versus the solar longitude (1950.0) in intervals of $0,1^\circ$. (Lindblad and Porubčan, 1994).

2.1.3. Characteristics of the New maximum

The basic characteristics of the new Perseid maximum are a relatively brief and near-constant duration of the outbursts as well as a high abundance of bright meteors (e.g. Shiba et al., 1993; Brown and Rendtel, 1996). Shiba et al. (1993), using photographic cameras, found a strong concentration of radiants within about $\pm 0,1^\circ$ during the 1991 outburst, observed in Japan. This means that the radiant area was much smaller than that observed so far. The limiting magnitude for the Perseid meteors is $\sim +1$ (-1 to -2 respectively, using lower sensitivity lenses). During the regular activity of the Perseids, such bright meteors are not frequently observed (usually $\sim 1/\text{hr}$). However, there was a case that more than 20 Perseid fireballs were recorded on a frame exposed for an hour during the outburst (Taguchi, 1991).

On the basis of the Perseids photographed in the European Fireball Network, Spurný (1995) studied the behaviour of potential groups of Perseids (the old and new) in the Earth's atmosphere. It is the only one possible test of different structure and composition of both groups of meteoroids. He has investigated how the beginning and terminal heights of new and regular Perseids depend on their initial masses. The Perseids used in that study were in the range from -5 to -13 maximum absolute magnitude, which corresponds to the range of initial masses from 1 g to 1 kg. He found that the dispersion of beginning and end heights is similar for all Perseids and independent of initial masses, especially for the beginnings. The average values of PE (the end height criterion defined in Ceplecha and McCrosky, 1976) are almost the same for both groups, though for

the new Perseids is somewhat lower and it could reflect that these meteoroids are slightly more friable on average.

It is evident that the strong activity in 1991 is different from the regular maximum of the Perseids. The peak (ZHR 300–500) at 16^h10^m UT corresponds to the solar longitude 138,9° (1950.0), which is close to the ascending node of the orbit of the parent comet. Marsden (1991) suggested that this activity may be associated with the return of the parent comet, which had been predicted on December 11th, 1992. Indeed, the comet passed the perihelion on December 12th, 1992 – just 1 day later.

These facts remind us the 1961 Leonid meteor shower, which preceded the return of Comet 55P/Tempel-Tuttle by more than 3 years. This shower was also rich on large meteoroids (McIntosh, 1973). A short duration of the activity is also worth noting. The duration of the showers depends generally on the age of the stream itself. As an exemplification of this claim can be a remarkable activity of Lyrids in the year 1982 (Porubčan et al., 1995).

Considering these characteristics, Wantanabe et al. (1993) suspected that this activity occurred due to the meteoroids recently ejected from the parent comet. The strong dust ejection from comet 109P/Swift-Tuttle at the previous return in 1862 is well known (Sekanina, 1981). This ejection could be the observable evidence of the release of a large amount of meteoroid particles, which encountered the Earth in recent years.

Jones and Brown (1996) found that the current activity of the Perseid stream is well represented by an ejection model using a cone angle about the comet-solar line of 90° and meteoroid density in the range of 400 – 800 kg m⁻³ (resp. interval of mass 1 – 10⁻⁵ g). They modelled the evolution in the distribution of the orbits of 1.5 × 10⁶ particles released at the 1862, 1737, and 1610 apparitions of 109P/Swift-Tuttle. The evolution of the stream is dominated by the influence of planetary perturbations, most notably those due to Jupiter and Saturn. A periodicity of approximately 12 years in Perseid activity is possible to be distinguished in the material ejected during the 1862 apparition. Without jovian perturbations, the nodes of the recently released Perseid particles would not cross the Earth's orbit. The activity from 1862 is notable in the simulations for 1991–1994 and also for the early 1980's. The weaker activity seen from 1987–1989 at large mass alone is exclusively due to the 1737 and 1610 ejecta with no contribution from the 1862 one. It is important to note that visual meteor data from the new peak included in a large number of bright meteors.

According to Jenniskens et al. (1998), a relatively brief and near-constant duration of the outbursts implies that the Earth crossed a ribbon-like structure of dust, which is extended more in the plane of the comet's orbit than perpendicular to it, and extends much further along the comet's orbit. They suggest that this ribbon-like structure is not caused by recent ejecta during the 1992 or 1862 returns of the comet. Instead, planetary perturbations must have had a time to disperse the stream significantly. They propose that these structures (the ribbon-like structure called Perseid Filament and Nodal Blanket) consist

of accumulations of the dust from tens of orbits, which have been accumulated near the comet position. They also concluded (Jenniskens et al., 1998) that the dust concentrated in the Nodal Blanket is protected from the close encounters with Jupiter due to the 1:11 mean motion resonance with this planet.

3. Crosswise structures

3.1. Data used

A fine structure of the Perseid stream and its filaments is studied using the method of indices – the procedure based only on mathematical statistics. In the study, the new completed 2003 version of the IAU MDC catalogue of precise photographic orbits (Lindblad et al., 2005) is applied. The previously published version was that of Lindblad and Steel (1994) in the Belgirate ACM proceedings.

The new IAU MDC catalogue consists of 4581 orbits derived from the photographic observations. There are 3 main differences between the new and older version of the catalogue:

1. the catalogue is containing new additional data on meteors and new reductions of the parameters obtained by original observers,
2. a smaller part of the data was improved by compilers,
3. all the data were transformed from the 1950.0 to the actual 2000.0 equinox.

The meteors with heliocentric velocities higher than 48 km s^{-1} were omitted from this analysis and thus the final set consisted of 4526 orbits.

3.2. Method of indices

The method of indices was used in the past to identify the major meteoroid streams at the IAU Meteor Data Center Lund catalogue of precise photographic orbits (Svoreň et al., 2000 – henceforth referred to as Paper 1). In that test run, all the major streams were identified, confirming the efficiency of the procedure. Besides the identification of the streams and associations, the method also enables a study of the fine structure of streams and their filaments. A separation of them by an iteration method is complicated and hardly realized. Firstly, we tested the efficiency of the procedure to study of the fine structure of a meteoroid stream three years ago (Svoreň et al., 2001). In this paper, a fine structure of the Perseid stream is studied applying the method of indices to the newest version of the photographic orbits database.

A detailed description of the method was published before in Paper 1. That is why we briefly highlight only basic ideas:

- as the input data, we used 5 orbital elements figuring in the Southworth-Hawkins D -criterion (1963), the coordinates of the radiant (which belong

to the most accurately known parameters) and the geocentric velocity (a significant parameter characteristic for physically related orbits),

- in the first step of procedure the relative ratios, approximated by small integers, corresponding to the reciprocal values of the relative errors, were applied as the basic numbers for the division of the parameters,
- next, indices to a meteor according to the interval pertinent to its parameters – see Fig. 4, are assigned on the basis of a division of the observed ranges of parameters,
- and, finally, a philosophy of the method says that a grouping of the meteors with the same indices reflects a similarity among the orbits – we introduce a term *group*.

The chosen number of intervals strongly influences the number of groups. We have to choose optimal numbers according to the numbers of orbits in individual groups.

3.3. Groups of similar orbits

The IAU Meteor Data Center Catalogue of precise photographic orbits (Lindblad et al., 2005) was used as a source of data. To select a basic set of data – Perseids, the method of indices was also used. Totally 875 orbits of Perseids were selected. The list of the selected Perseids is published currently in the Supplement to this number of *Contributions* (Svoreň and Kaňuchová, 2005).

On the basis of our previous results given in Paper 1, the individual numbers of intervals were used in the division of each parameter. The divisions were reciprocally proportional to the relative errors of parameters. This procedure homogenizes an infiltration of dispersed orbits of each group into neighbouring intervals. The errors of 8 individual parameters are determined as the root-of-mean-squares deviations from the mean values for the actually chosen 875 Perseids.

Table 1 lists:

- the parameters considered in the method of indices,
- the errors of the parameters for Perseid stream,
- the ranges – differences between the uppermost and lowest values of selected Perseids,
- the ratios of given ranges to the mean errors, which are moreover divided by the empirical value (2.04 in our case) fulfilling the condition of minimal sum of squares of differences between the real values and closest integers.
- The corresponding nearest integers serving as a basic set of numbers for the division of the parameters into the equidistant intervals (in the last row).

We introduce the term *association* for a group of meteors which contains minimally 3 similar orbits. We found, for the investigated Perseids, that basic

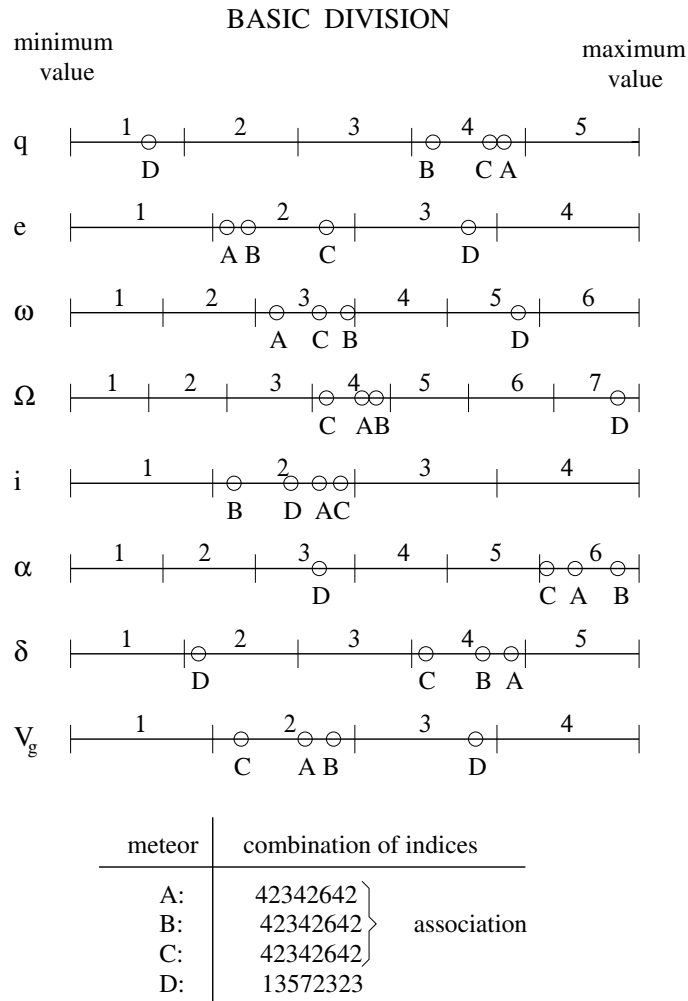


Figure 4. An example of assignment of indices for four meteors (A – D) according to the intervals of their eight parameters.

Table 1. The mean errors (MEs) and the numbers of intervals of basic division.

| parameter | <i>q</i> | <i>e</i> | ω | Ω | <i>i</i> | α | δ | <i>v_g</i> |
|---------------|----------|----------|----------|----------|----------|----------|----------|----------------------|
| ME | 0.021 | 0.14 | 6.5 | 4.7 | 2.6 | 7.1 | 1.8 | 1.8 |
| Range | 0.223 | 1.15 | 74.9 | 64.9 | 23.2 | 85.0 | 18.8 | 15.7 |
| Range/ME/2.04 | 5.20 | 4.02 | 5.65 | 6.77 | 4.37 | 5.87 | 5.12 | 4.27 |
| Intervals | 5 | 4 | 6 | 7 | 4 | 6 | 5 | 4 |

numbers of division of parameters (last row of Table 1) and its 2-multiple give very similar numbers of associations (53 and 57). We prefer the results obtained by using of 2-multiple of the basic numbers with a lower number of members (452 meteor orbits grouped into 57 associations) giving less dispersed orbits. Thus, we work with 57 associations numbered 1–57. The numbers of orbits in the associations differ between 3 (many cases) and 79 (association No. 23).

3.4. Structure of the Perseid meteoroid stream

A clustering of orbits in space means a clustering of their orbital parameters. If we deal with the associations of orbits, this is true for their mean parameters. In the previous paper dealing with the Perseid stream (Svoreň et al., 2001) the meaningful dependencies of their mean parameters on each other were looked for. The result is a finding that the dependencies $q = q(e)$, $q = q(\omega)$, and $\omega = \omega(\Omega)$ are sufficient to decide if particular associations are the components of a given clustering.

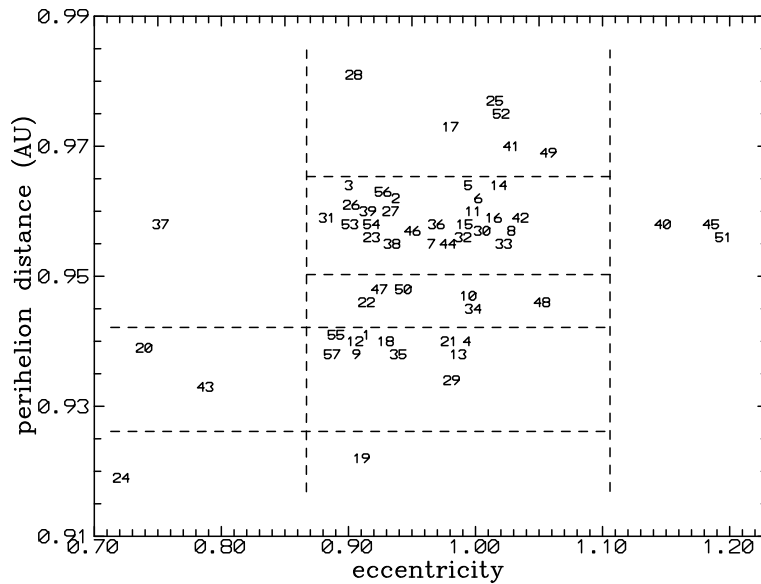


Figure 5. The dependence $q = q(e)$ for the associations selected. The associations are identified by their serial numbers. The position of given number corresponds to the mean values of q and e of the respective association.

The above mentioned dependencies with separated concentrations are plotted in Figs. 5–7. A clustering of associations in a single parameter can quite frequently occur as a coincidence. If a given set of associations really creates a

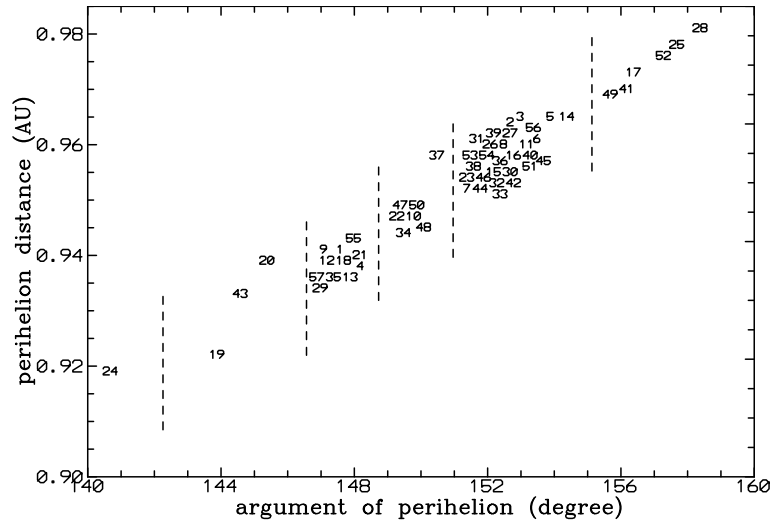


Figure 6. The dependence $q = q(\omega)$ for the associations selected. The associations are identified by their serial numbers. The position of given number corresponds to the mean values of q and ω of the respective association.

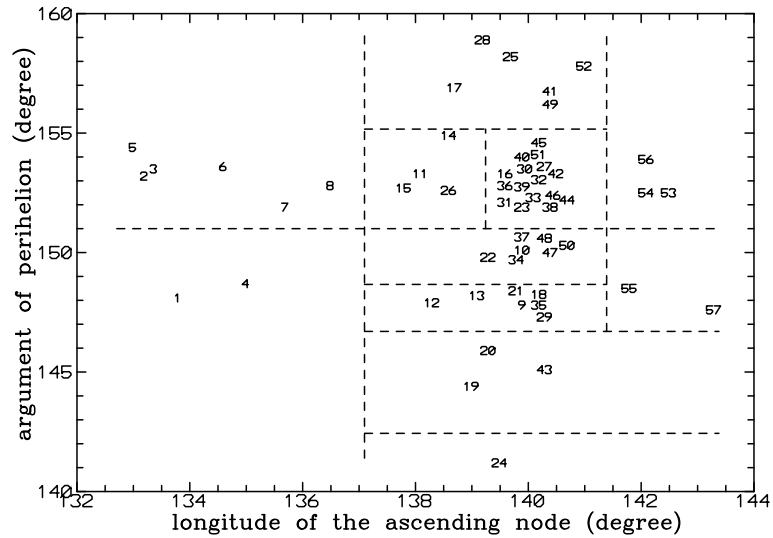


Figure 7. The dependence $\omega = \omega(\Omega)$ for the associations selected. The associations are identified by their serial numbers. The position of given number corresponds to the mean values of ω and Ω of the respective association.

cluster, then the clustering has to be observed in each parameter. Actually, the plots show that the associations have a tendency to create relatively isolated areas in the graphs. Almost all the associations detected within an area on one graph are also detected within one area on the other graphs.

A filament of the Perseid stream can be characterized by a mean parameter being very close to the boundary between two intervals of our division. In such a case, the appropriate index corresponds to both the neighbouring intervals, i.e. it is not unique and the filament is split into two associations. Or, it can be split into several associations, if more mean parameters of the filament are close to the appropriate boundaries of their divisions. The empirical limits among the filaments were obtained from the graphs and they are listed in Tab. 2.

Table 2. The empirical limits of parameters q , e , ω , and Ω separating the groups of associations. *d.r.* – designation of range.

| <i>d.r.</i> | <i>range</i> | <i>d.r.</i> | <i>range</i> | <i>d.r.</i> | <i>range</i> | <i>d.r.</i> | <i>range</i> |
|-------------|--------------|-------------|--------------|-------------|--------------|-------------|--------------|
| $q1$ | 0.916-0.926 | $e1$ | 0.712-0.864 | $\omega1$ | 140.5-142.3 | $\Omega1$ | 132.3-137.2 |
| $q2$ | 0.926-0.942 | $e2$ | 0.864-1.193 | $\omega2$ | 142.3-146.7 | $\Omega2$ | 137.2-139.2 |
| $q3$ | 0.942-0.950 | $e3$ | 1.193-1.536 | $\omega3$ | 146.7-148.8 | $\Omega3$ | 139.2-141.4 |
| $q4$ | 0.950-0.965 | | | $\omega4$ | 148.8-151.0 | $\Omega4$ | 141.4-145.4 |
| $q5$ | 0.965-0.985 | | | $\omega5$ | 151.0-155.1 | | |
| | | | | $\omega6$ | 155.1-158.6 | | |

The derived limits are, in the next step, used to search in the whole datafile of 875 Perseids, not only among 452 orbits assigned to one of the detected 57 associations. 560 (64%) of the Perseid orbits are selected to 17 filaments, which are listed in Tab. 3.

The mean eccentricity (the 8-th column) of the filament N is $\bar{e} > 1$. It is known that many of the Perseids (and another streams on retrograde orbits as well) have formally hyperbolic orbits (Kresák and Porubčan, 1970). This is obviously an effect of a large uncertainty of this element caused by a high geocentric velocity of the stream and following errors of measurements, resulting in a higher dispersion of the measured orbits. The range of eccentricity in our case even for mean orbits (highly smoothed values) is from 0.722 to 1.214. The high determined values indicate the high real values, but the corresponding real orbits are obviously elliptic.

The selected filaments are with a high probability real filaments of orbits in space (however, many of them are so small numerous that they fade in the field of all orbits). To support their real existence we note that each of the derived filaments consists of meteors observed in different years (see Fig. 8 which depicts how many meteors of filament M were observed in individual years).

It also means that the filaments do not represent any clustering of meteoroids in some positions on the orbit but long-time structures of the stream.

Table 3. The characteristics of the Perseid-stream filaments. *d.rs.* – designation of combination of range, *Q* – designation of filament, *N* – number of orbits.

| <i>d.rs.</i> | <i>Q</i> | <i>N</i> | α | δ | V_g | <i>q</i> | <i>e</i> | ω | Ω | <i>i</i> |
|--------------------------------|----------|----------|----------|----------|-------|----------|----------|----------|----------|----------|
| $\Omega 1, \omega 3, q 2, e 2$ | <i>A</i> | 15 | 43.3 | 57.9 | 58.70 | 0.937 | 0.971 | 147.7 | 135.1 | 111.4 |
| $\Omega 1, \omega 5, q 4, e 2$ | <i>B</i> | 36 | 39.3 | 56.8 | 59.27 | 0.958 | 0.981 | 152.7 | 134.4 | 112.5 |
| $\Omega 2, \omega 2, q 1, e 2$ | <i>C</i> | 7 | 50.0 | 57.7 | 58.61 | 0.921 | 0.907 | 143.9 | 138.9 | 113.2 |
| $\Omega 2, \omega 2, q 2, e 1$ | <i>D</i> | 8 | 47.3 | 57.4 | 56.56 | 0.935 | 0.744 | 144.9 | 139.1 | 111.9 |
| $\Omega 2, \omega 3, q 2, e 2$ | <i>E</i> | 10 | 48.0 | 59.2 | 58.39 | 0.936 | 0.959 | 147.6 | 138.7 | 110.7 |
| $\Omega 2, \omega 5, q 4, e 2$ | <i>F</i> | 23 | 44.3 | 57.8 | 59.45 | 0.959 | 0.985 | 153.0 | 138.3 | 113.0 |
| $\Omega 2, \omega 6, q 5, e 2$ | <i>G</i> | 10 | 42.3 | 57.3 | 59.35 | 0.974 | 0.958 | 157.0 | 138.7 | 113.3 |
| $\Omega 3, \omega 1, q 1, e 1$ | <i>H</i> | 3 | 49.7 | 57.7 | 56.10 | 0.917 | 0.722 | 140.7 | 139.5 | 111.5 |
| $\Omega 3, \omega 2, q 2, e 1$ | <i>I</i> | 7 | 49.7 | 57.5 | 57.35 | 0.931 | 0.795 | 144.7 | 140.1 | 112.8 |
| $\Omega 3, \omega 3, q 2, e 2$ | <i>J</i> | 53 | 50.0 | 57.8 | 59.05 | 0.936 | 0.933 | 147.5 | 140.1 | 113.6 |
| $\Omega 3, \omega 4, q 3, e 2$ | <i>K</i> | 47 | 48.9 | 58.0 | 59.45 | 0.945 | 0.975 | 149.7 | 140.0 | 113.4 |
| $\Omega 3, \omega 4, q 4, e 1$ | <i>L</i> | 5 | 45.9 | 57.3 | 57.04 | 0.956 | 0.762 | 150.1 | 139.9 | 112.4 |
| $\Omega 3, \omega 5, q 4, e 2$ | <i>M</i> | 242 | 47.1 | 57.9 | 59.32 | 0.956 | 0.958 | 152.2 | 140.0 | 113.3 |
| $\Omega 3, \omega 5, q 4, e 3$ | <i>N</i> | 21 | 48.5 | 57.5 | 62.84 | 0.956 | 1.214 | 153.7 | 140.0 | 115.8 |
| $\Omega 3, \omega 6, q 5, e 2$ | <i>O</i> | 40 | 45.1 | 57.4 | 60.01 | 0.971 | 0.993 | 156.4 | 140.2 | 114.3 |
| $\Omega 4, \omega 3, q 2, e 2$ | <i>P</i> | 17 | 53.8 | 58.3 | 59.07 | 0.936 | 0.927 | 147.4 | 142.8 | 113.7 |
| $\Omega 4, \omega 5, q 4, e 2$ | <i>R</i> | 16 | 50.1 | 58.3 | 59.20 | 0.957 | 0.939 | 152.5 | 142.3 | 113.5 |

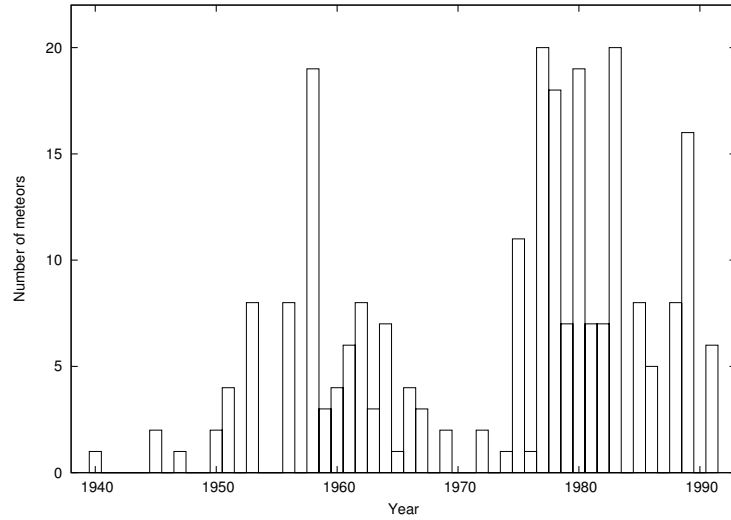


Figure 8. The amount of meteors belonging to the filament *M* in the individual years 1940–1990.

4. Filaments as part of complicated structures – branches

An analysis of the distribution of the selected filaments shows that part of them is not distributed in space accidentally, but they form higher structures, called here *the branches of meteoroid stream of Perseids*.

4.1. Time dependency

Different approaches to the analysis can be used. The simplest method is to investigate the dependence of an occurrence of filaments on the time scale represented by a value of the orbital ascending node Ω . We have to take into account that our filaments were found only in the densest part of the stream and the time from August 4 to 15 covers only a narrow interval from the total Perseid activity.

An activity curve of the Perseids – the whole interval and central part – is shown in Figs. 9 and 10. One can see positions of the mean orbits of 17 filaments.

The distribution of the mean orbits of filaments shows a well-known asymmetry of the activity around the maximum. The first period – beginning of the highest activity contains the filaments *B* and *A* (8 and 5 days before the maximum). The next period of maximum is characterized by double peaks (the day before the maximum – filaments *C* to *G*, the day of maximum – filaments *H* to *O*) and the last period is a rapid decrease of activity after the maximum – filaments *P* and *R* (3 days after). The plotted times are mean values of Ω of the filaments covering frequently almost 2 degree intervals.

Fig. 11 depicts the superposition of the activity of 17 Perseid filaments.

4.2. Positions of perihelia

The second possibility of the recovery of branches is to analyze the positions of perihelia of the filaments in the celestial sphere (see Fig. 12).

No grouping of the directions to the perihelion enables an unambiguous interpretation. It is very interesting that the perihelion directions are located in four zones:

- in the top-left zone – 2 filaments (*A* – *B*) from the period far prior the maximum,
- in the left-central zone – 5 filaments (*C* – *G*) with an activity 1 day prior the maximum,
- in the right-central zone – 8 filaments (*H* – *O*) active in the day of the maximum,
- in the down-right zone – 2 filaments (*P* – *R*) active after the maximum.

We have not succeed in finding any reasonable explanation of this distribution.

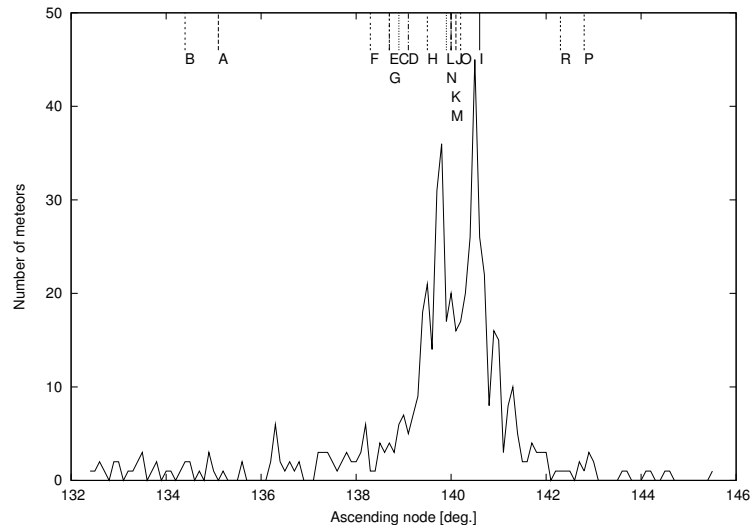


Figure 9. The activity curve of the Perseids – the whole interval.

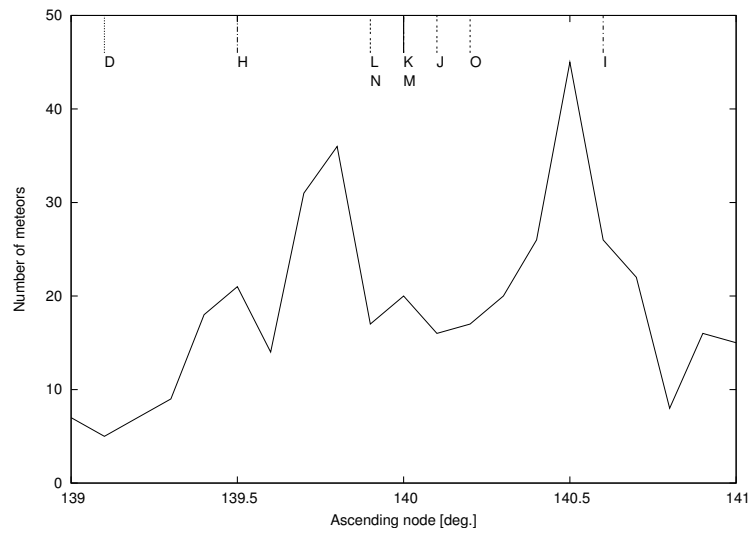


Figure 10. The activity curve of the Perseids – central part of event interval.

4.3. Distribution of radiant

An analysis of the distribution of the radiant of selected filaments is also naturally expected (see Fig. 13).

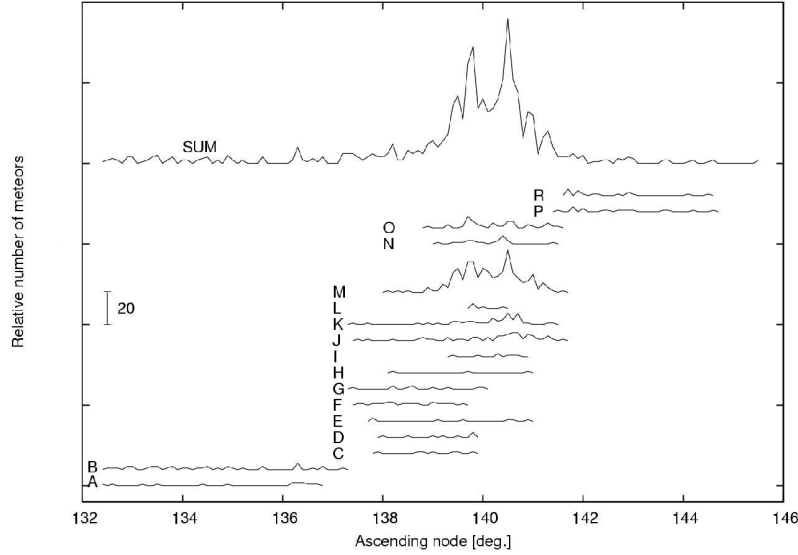


Figure 11. The activity profiles of 17 Perseid filaments and their superposition (SUM). The activity curves are vertically shifted from each other.

Besides a location of the group of low eccentric orbits (filaments *H*, *D*, *L* and *I*) at the lower part of the figure, further grouping of the other filaments has not been found. Of course, increase of declination and right ascension of the radiant with time is distinctly visible – those dependencies are expected as a known consequence of a motion of the radiant.

4.4. Space visualization

An analysis on the basis of a visualization of the space distribution of filaments gives many results.

We can distinguish following branches of filaments in Fig. 14:

- C1* – filaments *H*, *D*, *L*, *I*,
- C2* – filaments (*C*), *P*, *J*, (*R*),
- C3* – filaments (*G*), *M*, *E*,
- C4* – filaments *A*, *K*,
- C5* – filaments *B*, *F*.

Two filaments (*O*, *N*) at the *parabolic boundary* of the eccentricity interval seem to be individual structures without any connection with other filaments. According to a great uncertainty of the position of aphelia, they cannot be seriously classified. At branch *C2*, the filament *R* is relatively distant. Its classification as part of this branch is questionable. It is possible that the filaments of *C2* branch represent only a transition state between the *C1* and *C3* branches.

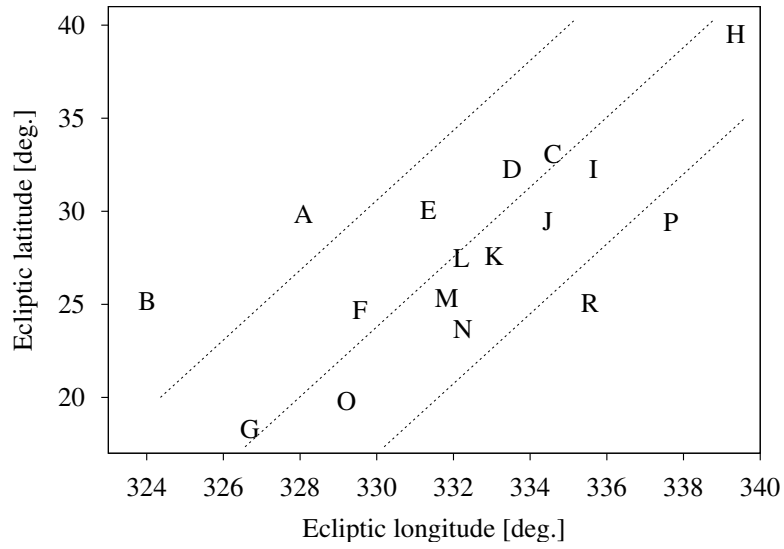


Figure 12. The positions of perihelia of 17 Perseid filaments in the ecliptic coordinate system.

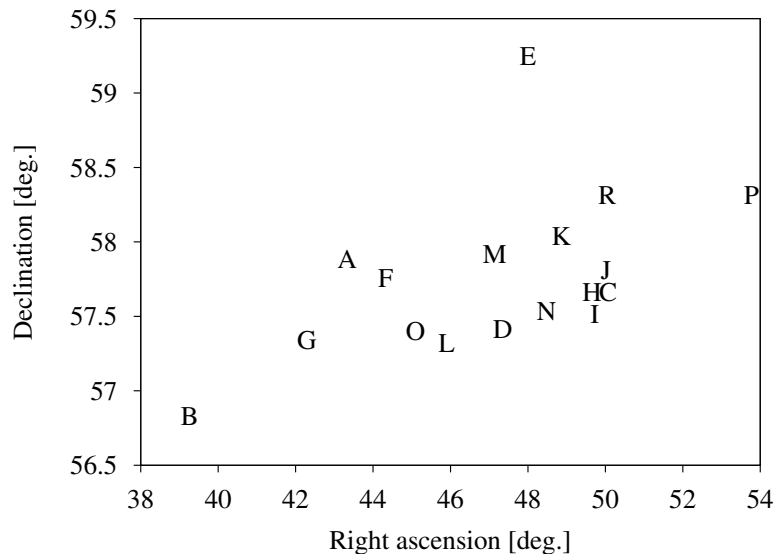


Figure 13. The positions of radiants of 17 Perseid filaments in the equatorial coordinate system.

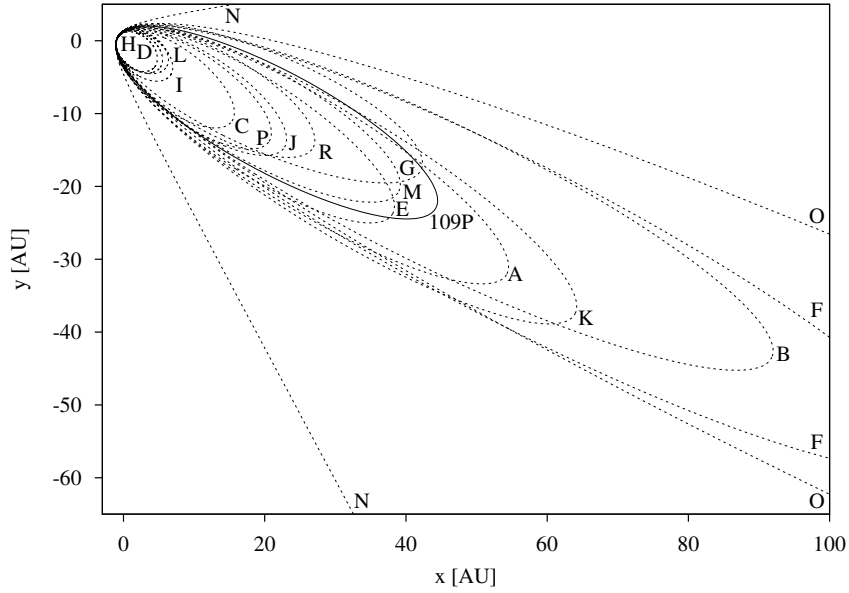


Figure 14. A projection the mean orbits of filaments into the plane of the mean orbit of 560 Perseids. The orbit of comet 109P/Swift-Tuttle in 1862 (Marsden and Williams, 1997) is considered. In the scale of the figure, there is no difference between that and the 1992 orbit.

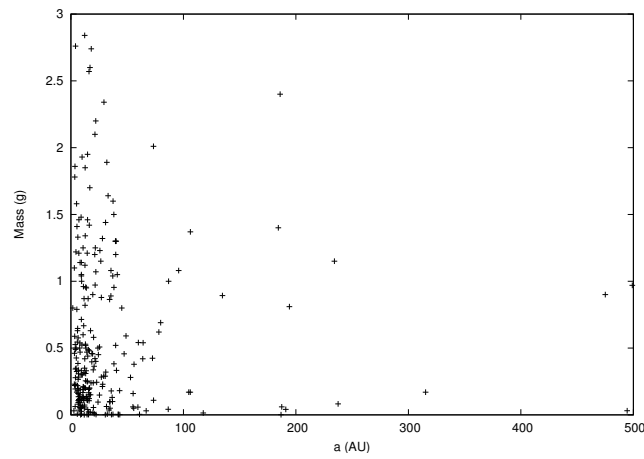


Figure 15. The meteoroid mass plotted as a function of the semimajor axis for Perseid stream meteoroids with $e < 1$ and $m < 3$ g.

We have to take into account that our conclusions are considerably influenced by the positions of aphelia closely connected with an eccentricity – a parameter with the largest errors in the database. On the other hand, clustering of the aphelia could hardly be connected with the low precision of determination of the meteor velocity.

By the analysis of the photographics Perseid meteor orbital data, the semi-major axis of causative meteoroids is found not to vary systematically as a function of meteoroid mass over the mass range $0,001 < m < 30$ g (Harris and Hughes, 1995). The same results (Fig. 15) are obtained in our study of Perseids with known mass and elliptic orbits (what is 333) picked up from the newest version of IAU MDC database.

4.5. D -discriminant analysis

In the last analysis of the filamentary structure, D -discriminants of all the pairs of selected filaments were calculated (Tab. 4).

Table 4. The values of D -discriminant (multiplied by 100) among the mean orbits of filaments.

| | B | C | D | E | F | G | H | I | J | K | L | M | N | O | P | R |
|---|----|----|----|----|----|----|----|----|----|----|----|----|----|----|----|----|
| A | 10 | 13 | 24 | 7 | 9 | 15 | 29 | 21 | 10 | 9 | 22 | 10 | 28 | 16 | 15 | 13 |
| B | | 21 | 29 | 14 | 7 | 9 | 34 | 26 | 16 | 13 | 25 | 10 | 26 | 10 | 21 | 15 |
| C | | | 17 | 9 | 18 | 23 | 19 | 11 | 6 | 12 | 17 | 14 | 36 | 22 | 7 | 14 |
| D | | | | 22 | 27 | 28 | 6 | 6 | 19 | 24 | 7 | 24 | 50 | 31 | 20 | 23 |
| E | | | | | 11 | 17 | 26 | 18 | 6 | 6 | 20 | 9 | 29 | 16 | 9 | 10 |
| F | | | | | | 7 | 33 | 24 | 12 | 8 | 23 | 5 | 24 | 6 | 16 | 9 |
| G | | | | | | | 34 | 26 | 17 | 14 | 23 | 9 | 27 | 5 | 20 | 12 |
| H | | | | | | | | 9 | 24 | 29 | 13 | 29 | 54 | 36 | 23 | 28 |
| I | | | | | | | | | 15 | 20 | 9 | 20 | 45 | 27 | 14 | 18 |
| J | | | | | | | | | | 6 | 18 | 8 | 31 | 16 | 5 | 8 |
| K | | | | | | | | | | | 21 | 5 | 25 | 12 | 9 | 6 |
| L | | | | | | | | | | | | 20 | 46 | 25 | 18 | 18 |
| M | | | | | | | | | | | | | 26 | 8 | 11 | 4 |
| N | | | | | | | | | | | | | | 23 | 32 | 28 |
| O | | | | | | | | | | | | | | | 19 | 10 |
| P | | | | | | | | | | | | | | | | 9 |

On the basis of similarity of orbits expressed by the low values of D , a check of the reality of branches found in the previous section is done. The process of the check by a D -criterion does not confirm that the filament G belongs to the branch $C3$. Mean orbits of all other members of branches are very similar to each other within a given branch. This implies a possibility of their similar dynamical evolution. The branches found from the analysis of D -values:

V1 – the filaments *H*, *D*, *I*, and *L* – a very compact group of relatively low eccentric orbits also found by previous methods (= *C1*),
V2 – the filaments *C*, *J*, and *P* – agreement with the method of space visualization (= *C2* without the problematic *R* filament),
V3 – a central part of the stream – the filaments *A*, *E*, *K*, *M*, *R*, *F*, *B* (*C3* + *C4* + *C5* + filament *R*, without the problematic filament *G*),
V4 – the filaments *O* and *G* – a very interesting pair, which originates on the basis of small differences between angle parameters of the orbits,
V5 – the individual filament *N* – the hyperbolic mean orbit with the highest eccentricity; all the $D \geq 0.23$. The high values of D among the *N* and all other filaments could indicate that this filament is well separated in the stream. On the other side, the high values of D could be a consequence of a low transition probability into these (hyperbolic) orbits. If it is true, the filament *N*, as a structure, does not really exist and it has been extracted just due to large errors of velocity measurements.

The analysis using the D -criterion results in 1 individual filament (*N*), 3 branches – *V1* (*H*, *D*, *I*, *L*), *V2* (*C*, *J*, *P*), *V4* (*O*, *G*), and the dense kernel of the Perseid stream – *V3* (*A*, *B*, *E*, *F*, *K*, *M*, *R*) containing 7 filaments in total. Branches *C3* (*E*, *M*), *C4* (*A*, *K*) and *C5* (*B*, *F*) found from the visualization of the space distribution of the orbits are submerged into the dense central part of the Perseid stream – *V3*.

The particles of the *M* filament move in orbits very similar to the comet's one. That is why the transits into these orbits are very likely. There are just a small differences among the branches obtained by visualization of the space distribution (seen in Fig. 14) and that obtained by using the D -criterion (similar orbits). In addition, these differences occurred only in the densest central part of the stream. This finding cannot be understood as any discrepancy. The structures derived by the visualization are a display of a current resonance frame; D -discriminant values qualify the transition probability to the resonance stage. Moreover, resonance orbits are preferred, because the concentration of meteoroid orbits is enhanced gradually with time. Thus, the number of meteoroids moving in orbits similar to that of resonances tend to be higher than expected on the basis of energetic transition probability. In Fig. 16, an evolution diagram of the filaments is shown. It displays the most probable transits (of meteoroids) between the filaments, implied by the minimal values of D for each considered filament.

4.6. A global view of the Perseid stream structure

The combination of both the above-used methods gives us the following big picture of the stream:

We have separated and analysed the set of 875 photographic Perseids. 560 individual orbits are concentrated into 17 individual filaments. The selected filaments are not distributed in space accidentally, but they form higher structures

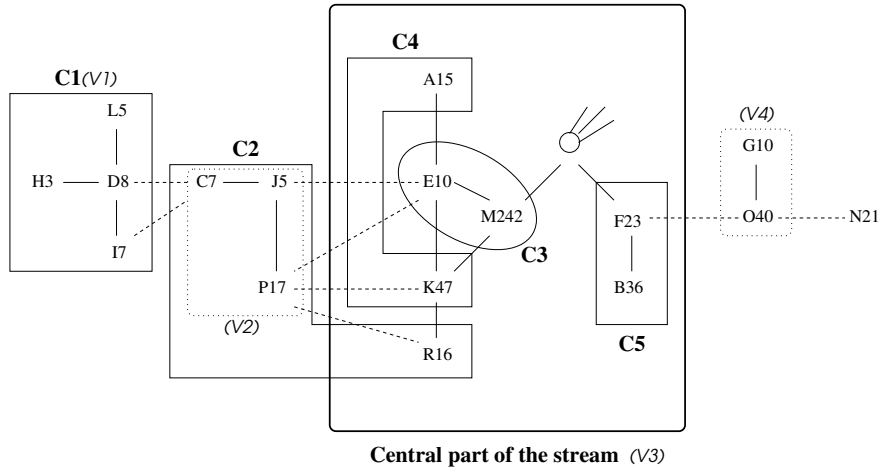


Figure 16. The scheme demonstrating the relationships among the mean orbits of the filaments as well as the orbit of the parent comet. Concerning an individual filament, only the most likely, minimum- D -value coupling is drawn. Continuous lines represent plausible transitions; dashed lines that less likely but real ones. There are written numbers of allocated orbits of individual filaments. One can see that the number of orbits of filaments strengthen a low probability of distinct transitions, e.g. the orbits with short period and small eccentricity (branch containing H , D , I and L filaments) are filled up essentially less than orbits of filaments composing the central part of the stream.

consisting of 1 individual filament, 3 branches of the stream containing 9 filaments altogether, and a central part of the stream. In the central part of Perseids, 3 branches and 1 individual filament were identified. The structures are divided into a cloud of 315 dispersed orbits.

The structure of filaments and branches is shown in Fig. 17.

5. Resonance structures

5.1. Encounter geometry

The mean perihelion distance of Perseids in our sample is $q = 0,951 \pm 0,021$ AU. None of observed Perseids has $q > 1.014$ AU. This threshold value could be a consequence of the real distribution of perihelion distances in the stream, or simply the boundary of a sampling interval (impossibility to observe the meteoroids with the perihelion distance greater than the heliocentric distance of the Earth during Perseid activity). Using similar data and analysis, as well as their original model, it has been found by Harris et al. (1995), that the Earth only samples the *inner edge* of the Perseid stream and that the core of the

Table 5. The orbital parameters of 109P/Swift-Tuttle and of the Perseid meteoroid stream. Source (*So.*): (1) Yau, Yeomans and Weissman (1994), (2) Whipple (1938), (3) Ceplecha (1951), (4) Hawkins and Almond (1952), (5) Cook (1973), (6) Harris and Hughes (1995), (7) this paper (weighted mean orbit of 560 meteors).

| | <i>T</i> | <i>e</i> | <i>q</i> (AU) | ω (deg) | Ω (deg) | <i>i</i> (deg) | <i>P</i> (y) | <i>So.</i> |
|----------|------------|----------|---------------|----------------|----------------|----------------|--------------|------------|
| 69 BC | Aug. 27.10 | 0.961 | 0.980 | 152.4 | 139.9 | 113.9 | 127.9 | 1 |
| 188 AD | Jul. 10.55 | 0.962 | 0.977 | 152.6 | 139.3 | 113.9 | 130.3 | 1 |
| 1737 II | Jun. 15.85 | 0.961 | 0.980 | 152.7 | 139.5 | 113.7 | 127.8 | 1 |
| 1862 III | Aug. 23.42 | 0.963 | 0.963 | 152.8 | 139.4 | 113.6 | 131.7 | 1 |
| 1992t | Dec. 12.32 | 0.964 | 0.958 | 152.0 | 139.4 | 113.4 | 135.0 | 1 |
| 2126 | Jul. 12.41 | 0.964 | 0.956 | 152.1 | 139.6 | 113.4 | 136.2 | 1 |
| Perseids | | 0.958 | 0.968 | 152.6 | 141.5 | 119.7 | 109.5 | 2 |
| | | 0.947 | 0.947 | 150.9 | 149.4 | 112.2 | 77.1 | 3 |
| | | 0.93 | 0.97 | 153 | 139.5 | 114 | 54.6 | 4 |
| | | 0.965 | 0.953 | 151.5 | 139 | 113.8 | 148.2 | 5 |
| | | 0.969 | 0.949 | 150.8 | 138.8 | 113.1 | 169.4 | 6 |
| | | 0.962 | 0.952 | 151.3 | 139.6 | 113.3 | 125.4 | 7 |

| | | |
|----------------------------|-------------|------------|
| branch H, D, I, L | 23 orbits | |
| branch C, P, J | 77 orbits | |
| Central part of the stream | filament R | 16 orbits |
| | branch E, M | 252 orbits |
| | branch A, K | 62 orbits |
| | branch B, F | 59 orbits |
| branch O, G | 50 orbits | |
| filament N | 21 orbits | |

Figure 17. The order of the structures at this picture is from low-eccentric to formally hyperbolic orbits.

descending nodal distribution of the actual Perseids extends out to heliocentric distances of at least 1.2 AU. In order to reach this conclusion, the orbit of the Perseid parent comet 109P/Swift-Tuttle has been integrated backwards in time over a period of 270 000 years. Only over the last 160 000 years has the decay of this comet led to the production of any Perseid meteoroids that can be observed from Earth.

5.2. Approaches of the stream to planets and planetary perturbations

There are elements of mean (weighted) orbit of 560 meteors concentrated into 17 individual filaments in the last row of Tab. 5. The positions of the nodes of Perseid stream's mean orbit are interesting: descending one near the Earth's orbit in 1 AU, ascending one behind the orbit of Saturn, almost 12 AU from the Sun. Between these nodes, the distance of the orbit from the ecliptic plane does not increase more than 1.74 AU (see Fig. 18). Hence, although meteoroids are at large distances from both the nodes, they pass near the orbits of Mars, Jupiter, and Saturn, which perturb their orbits. The perturbation power is proportional to the planet's mass and reciprocally proportional to the square of distance of a perturbed body. The maximum amplitudes of the perturbative force of individual planets are listed in Tab. 6

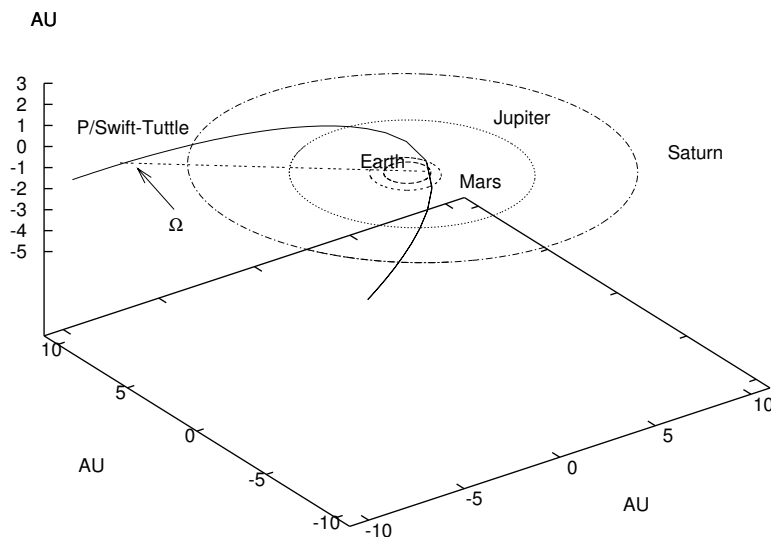


Figure 18. The orbit of the Perseid parent comet and the orbits of Earth, Mars, Jupiter, and Saturn.

We can expect that the Perseid stream's dynamics is controlled mostly by giant planets. As seen from Table 6, the perturbative forces from Jupiter and Saturn much exceed those from the other giant planets. The magnitude of perturbative force from Uranus is one percent of that of Saturn, and that from

Neptune is just a thousandth of Saturn's one. More than two-times stronger influence of Saturn compared to that of Jupiter stems from the diminishing distance of the stream mean orbit (or the parent comet's orbit) from the orbital plane of jovian planets as it is gradually closer and closer to its ascending node (which lies relatively close to the Saturn's orbit).

Table 6. The planetary disturbing forces. M – the mass of the planet; the mass of Saturn chosen as a unit; R_{min} – the minimal distance between the mean orbit of the Perseid stream (last row of Tab. 5) and a given orbit of the planet; F – the maximal disturbing force of the planet; the force of Saturn chosen as a unit.

| Planet | M (Saturn=1) | R_{min} [AU] | F (Saturn=1) |
|---------|----------------|----------------|----------------|
| Jupiter | 3.341 | 1.472 | 0.574 |
| Saturn | 1.000 | 0.610 | 1.000 |
| Uran | 0.152 | 2.382 | 0.010 |
| Neptun | 0.181 | 7.295 | 0.001 |

5.3. Resonance gaps in the distribution of semimajor axes of Perseids

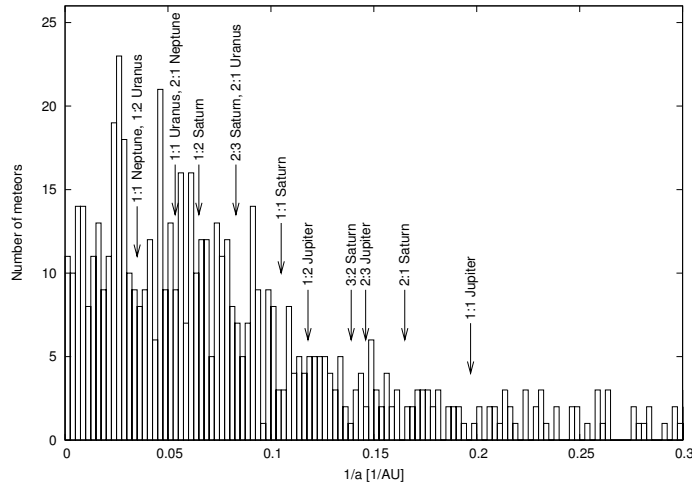


Figure 19. The distribution of $1/a$ – interval of $1/a$ division of 0.0025 AU^{-1} . The locations of mean-motion resonances as suggested by Wu and Williams (1995) are marked.

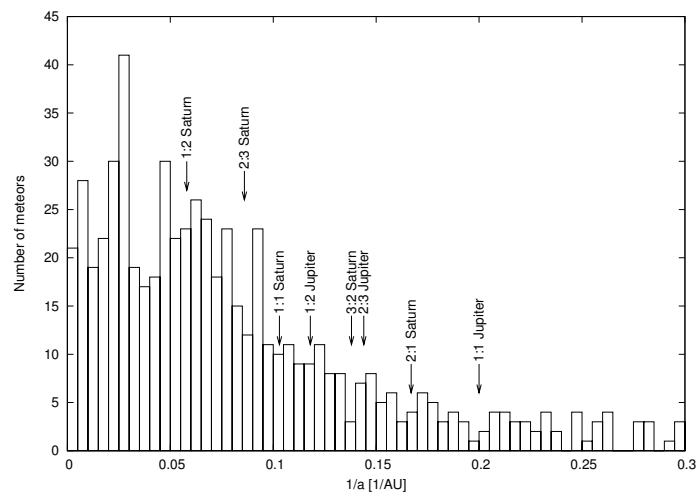


Figure 20. The distribution of $1/a$ – interval of $1/a$ division of 0.005 AU^{-1} . The locations of general mean-motion resonances are marked.

Wu and Williams (1995) found gaps in the distribution of the reciprocal semimajor axes of Perseid meteoroids. They associated them with the mean-motion resonances of Jupiter, Saturn, Uranus, and Neptune. The photographic orbits of 442 Perseids extracted from the previous version of the IAU MDC Catalogue were studied.

We carry out the comparison of the theoretical resonance positions with the detected diminutions of Perseid numbers again, using the considerably more numerous database. We study 648 Perseids (for which $1/a > 0$) selected from the newest version of the database. In the analysis, we use the $1/a$ division equal to that of Wu and Williams, at first. Despite an essentially larger amount of considered orbits, the gaps are not well-marked, in our opinion (see Fig. 19). But, as it can be seen in Fig. 20, the gaps are deeper (relatively to neighbouring intervals) when the division of $1/a$ with the larger interval of 0.005 AU^{-1} is used.

Only the strongest resonances with Jupiter (1:1, 2:3, and 1:2) and Saturn (2:1, 3:2, 1:1, 2:3, and 1:2) are identified with no doubt. We have no reasonable resonance explanation of some gaps occurring in the distribution, e.g. the gap at $1/a = 0.098 \text{ AU}^{-1}$. Some coincidences seem to appear just by chance with respect to the magnitude of the disturbing force of Uranus and Neptune.

We note that a substantially shortened version (because of a lack of space) containing our results on filaments and branches of Perseids was presented at Meteoroids 2004 Conference in London, Canada and is published now in the Earth, Moon and Planets (Svoreň et al., 2005).

Acknowledgements. This research was supported by VEGA - the Slovak Grant Agency for Science (grant No. 4012).

References

- Brown, P., Rendtel, J.: 1996, *Icarus* **124**, 414
- Cook, A.F.: 1973, in *Evolutionary and Physical Properties of Meteoroids*, eds.: C.L. Hemenway, P.M. Millman and A. F.Cook, NASA, Washington, 183
- Cepelcha, Z.: 1951, *Bull. Astron. Inst. Czechosl.* **2**, 114
- Cepelcha, Z., McCrosky, R.E.: 1976, *J. Geophys. Res.* **81**, 6257
- Evans, S.: 1990, *J. British Astron. Assoc.* **100**, 4
- Green, D.W.E.: 1993, *Int. Comet. Quart.* **15**, 182
- Harris, N.W., Hughes, D.W.: 1995, *Mon. Not. R. Astron. Soc.* **273**, 992
- Harris, N.W., Yau, K.K.C., Hughes, D.W.: 1995, *Mon. Not. R. Astron. Soc.* **273**, 999
- Hasegawa, I.: 1993, in *Meteoroids and their Parent Bodies*, eds.: I.P. Williams and J. Štohl, Ast. Inst. Slovak Acad. Sci., Bratislava, 207
- Hawkins, G.S., Almond, M.: 1952, *Mon. Not. R. Astron. Soc.* **112**, 219
- Hughes, D.W.: 1990, *Mon. Not. R. Astron. Soc.* **245**, 198
- Jenniskens, P.: 1994, *Astron. Astrophys.* **287**, 990
- Jenniskens, P.: 1995, *Astron. Astrophys.* **295**, 206
- Jenniskens, P., Betlem, H., de Lignie, M., ter Kuile, C., van Vliet, M.C.A., van 't Leven, J., Koop, M., Morales, E., Rice, T.: 1998, *Mon. Not. R. Astron. Soc.* **301**, 941
- Jones, J., Brown, P.: 1996, *ASP Conf. Ser.* **104**, 105
- Kronk, G.W.: 1988, *Meteor showers: A descriptive Catalogue*, Enslow, Hillside
- Koschack, R., Roggemans, P.: 1991, *WGN, J. Int. Meteor Org.* **19**, 87
- Kresák, L', Porubčan, V.: 1970, *Bull. Astron. Inst. Czechosl.* **21**, 153
- Lindblad, B.A.: 1986, in *Asteroids, Comets, Meteors II*, eds.: C.I. Lagerkvist, B.A. Lindblad, H. Lundstedt and H. Rickman, Uppsala Univ., Uppsala, 531
- Lindblad, B.A.: 1987, in *The Evolution of the Small Bodies of the Solar System*, eds.: M. Fulchignoni and L'. Kresák, Soc. Italiana Fis., Bologna, 229
- Lindblad, B.A., Neslušan, L., Porubčan, V., Svoreň, J.: 2005, *Earth, Moon, Planets* **93**, 249
- Lindblad, B.A., Porubčan, V.: 1994, *Planet. Space Sci.* **42**, 117
- Lindblad, B.A., Steel, D.I.: 1994, in *IAU Coll. 160*, eds.: A. Milani, M. DiMartino and A. Cellino, Kluwer Acad. Publ., Dordrecht, 497
- Marsden, B.G.: 1991, *IAU Circ.* 5330
- Marsden, B.G., Williams, G.V.: 1997, *Catalogue of Cometary Orbits*, Smiths. Astrophys. Obs., Cambridge
- McIntosh, B.A.: 1973, in *Evolutionary and Physical Properties of Meteoroids*, eds.: C.L. Hemenway, P.M. Millman and A.F.Cook, NASA, Washington, 193
- Olson, D.W.: 1992, *Meteor News* **98**
- Porubčan, V., Štohl, J., Svoreň, J.: 1992, *Contrib. Astron. Obs. Skalnaté Pleso* **22**, 25
- Roggemans, P.: 1989, *WGN, J. Int. Meteor Org.* **17**, 127
- Sekanina, Z.: 1981, *Astron. J.* **86**, 1741
- Shiba, Y., Ohtsuka, K., Wantanabe, J.: 1993, in *Meteoroids and their Parent Bodies*, eds.: I.P. Williams and J. Štohl, Ast. Inst. Slovak Acad. Sci., Bratislava, 189

- Southworth, R.B., Hawkins, G.S.: 1963, *Smithson. Contrib. Astrophys.* **7**, 261
- Spurný, P.: 1995, *Earth, Moon, Planets* **68**, 529
- Svoreň, J., Kaňuchová, Z.: 2005, *Contrib. Astron. Obs. Skalnaté Pleso* **35**, 199
- Svoreň, J., Neslušan, L., Kaňuchová, Z., Porubčan, V.: 2005, *Earth, Moon, Planets*, in press
- Svoreň, J., Neslušan, L., Porubčan, V.: 1997, *Planet. Space Sci.* **45**, 557
- Svoreň, J., Neslušan, L., Porubčan, V.: 2000, *Planet. Space Sci.* **48**, 933
- Svoreň, J., Porubčan, V., Neslušan, L.: 2001, in *Proc. Meteoroids 2001 Conf. ESA SP-495*, ed.: B. Warmbein, ESA Publ. Div., ESTEC, Noordwijk, 105
- Šimek, M.: 1987, *Bull. Astron. Inst. Czechosl.* **38**, 1
- Watanabe, J.: 1993, in *Meteoroids and their Parent Bodies*, eds.: I.P. Williams and J. Štohl, Astron. Inst. Slovak Acad.Sci., Bratislava, 197
- Taguchi, U.: 1991, *Yamamoto Circ.* 2170 (in Japanese)
- Whipple, F.L.: 1938, *Proc. Am. Phil. Soc.* **79**, 499
- Williams, I.P.: 1997, *Mon. Not. R. Astron. Soc.* **292**, L37
- Williams, I.P., Wu, Z.: 1994, *Mon. Not. R. Astron. Soc.* **269**, 524
- Wright, F.W., Whipple, F. L.: 1953, *Astron. J.* **58**, 49
- Wu, Z., Williams, I.P.: 1995, *Mon. Not. R. Astron. Soc.* **276**, 117
- Yau, K., Yeomans, D., Weissman, P.: 1994, *Mon. Not. R. Astron. Soc.* **266**, 305
- Zvolánková, J.: 1984, *Contrib. Astron. Obs. Skalnaté Pleso* **12**, 45